Available online at www.sciencedirect.com

ScienceDirect

International Journal of Heat and Mass Transfer 50 (2007) 4805–4811

International Journal of HEAT and MASS TRANSFER

www.elsevier.com/locate/ijhmt

Improvement on device performance in multi-pass heat transfer through a parallel-plate channel with external recycle

Chii-Dong Ho *, Yu-Chuan Tsai, Jr-Wei Tu

Department of Chemical and Materials Engineering, Tamkang University, Tamsui, Taipei 251, Taiwan, ROC

Received 27 June 2006; received in revised form 1 March 2007
Available online 3 May 2007

Abstract

A new external-recycle device of multi-pass heat exchangers with uniform wall temperature, resulting in a considerable heat-transfer efficiency improvement, has been designed and studied theoretically. The theoretical analysis on the temperature profile and heat-transfer efficiency improvement has been developed by using an eigenfunction expansion in power series. The analytical predictions are represented graphically and compared with that in single-pass devices and the previous work [C.D. Ho, H.M. Yeh, Y.C. Tsai, Improvement in performance of multi-pass laminar counterflow heat exchangers with external refluxes, Int. J. Heat Mass Transfer 45 (2002) 3529–3547]. A substantial heat-transfer efficiency improvement is obtained by employing such a new recycle type with a suitable adjustment of the impermeable-sheet position and recycle ratio, instead of using the single-pass device without external recycle for $Gz > 10$ and the recycle type of the previous study for $Gz > 30$.

Keywords: Heat exchangers; Conjugated Graetz problems; Multi-pass operations; External recycle

1. Introduction

The problem dealing with the laminar heat and mass transfer in a bounded conduit under constant wall temperature or heat flux is the well-known classical Graetz problem [1–5], and the analytical solution to such a classical Graetz problem is solved with the assumptions of fully-developed laminar flow and no axial heat conduction. Actually, the axial heat conduction can not be neglected for the liquid metal (low Prandtl number fluids) or viscous fluids (small Reynolds number flows). The extension of the classical Graetz problem with considering the axial heat conduction is so-called the extended Graetz problem [6–10]. However, both the classical and extended Graetz problems focus on the systems with only one single-stream and single-phase heat or mass transfer. However, the heat or mass transfer problems of multi-stream or multi-phase are widely used in industrial processes. The conjugated Graetz problems [11–15] are referred to the analysis of two or more adjacent streams or phases of multi-stream or multi-phase problems coupled through mutual conditions at the boundaries.

In practice, there are three strategies to enhance the heat or mass transfer rate: dividing an open-duct device into several subchannels [16,17], reducing the channel size [18,19] and introducing the external or internal recycle concept into design [20,21]. In chemical industrial processes, the recycle-effect concept is widely used in designing separation processes and chemical reactors, such as bioreactors [22], filters [23], gas absorbers [24], thermal diffusion [25] and air-lift reactor [26]. Base on these strategies, the present study combines the concepts of dividing an open-duct device into several subchannels with adding the external recycle to improve the heat-transfer efficiency.

The heat transfer problem in a parallel-plate channel has been studied in many researches [27–30]. The present work

* Corresponding author. Tel.: +886 2 26215656x2724; fax: +886 2 26209887.
E-mail address: cdho@mail.tku.edu.tw (C.-D. Ho).

0017-9310/$ - see front matter © 2007 Elsevier Ltd. All rights reserved.
doi:10.1016/j.ijheatmasstransfer.2007.03.010

Nomenclature

B	conduit width, m
D_e	equivalent diameter of the conduit, m
F_m	eigenfunction associated with eigenvalue λ_m
f	friction factor
Gz	Graetz number, $2VW/\alpha BL$
$\bar{h}$	average heat transfer coefficient, kW/m K
I_{h1}	heat-transfer efficiency improvement based on single-pass devices, defined by Eq. (30)
I_{h2}	heat-transfer efficiency improvement based on the previous work [31], defined by Eq. (31)
I_p	power consumption increment of, defined by Eq. (33)
L	conduit length, m
ℓw_f	friction loss in conduit, N m/kg
$\overline{Nu}$	average Nusselt number
P	power consumption, N m/s
R	recycle ratio
Re	Reynolds number
S_m	expansion coefficient associated with eigenvalue λ_m
V	input volume flow rate of conduit, m^3/s
v	velocity distribution of fluid, m/s
$\bar{v}$	average velocity of fluid, m/s
W	distance between two parallel plates, m
x	transversal coordinate, m
z	longitudinal coordinate, m

Greek symbols

α	thermal diffusivity of fluid, cm^2/s
β	ratio of channel thickness, $W_a/W_b = W_d/W_c$
ξ	longitudinal coordinate, z/L
η	transversal coordinate, r/R
θ	dimensionless temperature, $(T - T_I)/(T_s - T_I)$
λ_m	eigenvalue
μ	fluid viscosity, kg/m s
ρ	fluid density, kg/m^3
ψ	dimensionless temperature, $(T - T_s)/(T_I - T_s)$

Subscripts

A	the channel a in double-pass devices
a	the channel a in multi-pass devices
B	the channel b in double-pass devices
b	the channel b in multi-pass devices
c	the channel c in multi-pass devices
D	double-pass device
d	the channel d in multi-pass devices
F	at the outlet
I	at the inlet
L	at the end of the channel
0	in a single-pass device without recycle
prev.	the data of the previous work [31]
s	at the wall surface

is an extension of our previous work [31] except the recycle type. As referred to the conclusions of previous work [31], one can find that the application of multi-pass and recycle concepts can readily improve the heat transfer efficiency of the parallel-plate heat exchangers. In this study, a new and more effective external recycle type has been designed to achieve further improvement of the heat transfer efficiency in the parallel-plate heat exchangers as compared with that in the previous work [31]. The temperature profile of fluid and the heat-transfer efficiency improvement has been investigated theoretically by using orthogonal expansion techniques [32–35] in terms of an extended power series. The purposes of this work are to design a new and more effective recycle design, to formulate the mathematical statement for obtaining an analytical solution of the present conjugated Graetz problem and to find the optimal operating conditions. This study also discusses the heat-transfer efficiency improvement of such a multi-pass heat exchanger with external recycle by comparing with that of the single-pass devices and our previous work [31].

2. Temperature profiles

A multi-pass heat exchanger was obtained by inserting three barriers with negligible thermal resistance into a parallel-plate channel with thickness W, length L, and width B ($\gg W$) to divide the open duct into four parts, subchannel a, b, c and d with thickness W_a, W_b, W_c and W_d, respectively, and the channel thickness ratio is defined as $\beta = W_a/W_b = W_d/W_c$. The wall temperatures of the multi-pass heat exchanger are kept constant as T_s. Before entering two outlet conduits, the feed will premixed with the fluid exiting from the inner conduits with volume flow rate RV and the outlet temperature T_F as shown in Fig. 1.

The velocity profiles in the four subchannels of present multi-pass devices were redefined, respectively, as follows:

$$v_a(\eta_a) = \frac{(R+1)V}{BW_a}(6\eta_a - 6\eta_a^2) \tag{1}$$

$$v_b(\eta_b) = \frac{-(R+1)V}{BW_b}(6\eta_b - 6\eta_b^2) \tag{2}$$

$$v_c(\eta_c) = \frac{-(R+1)V}{BW_c}(6\eta_c - 6\eta_c^2) \tag{3}$$

and

$$v_d(\eta_d) = \frac{(R+1)V}{BW_d}(6\eta_d - 6\eta_d^2) \tag{4}$$

The first term of the right-hand side of Eqs. (1)–(4) represents the average velocity in each subchannel. The velocity profiles of the present work, as show in Eqs. (1)–(4), are different to those of the previous work [31]. The governing

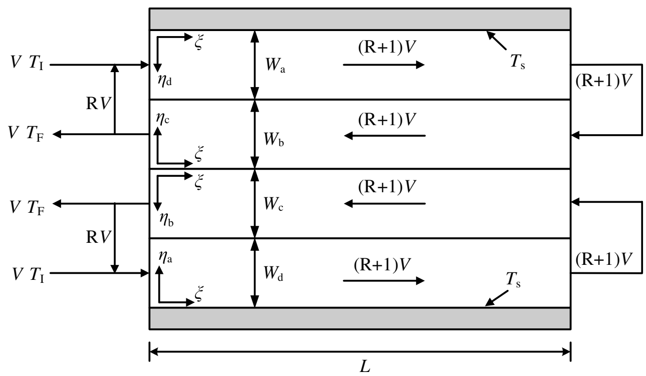

Fig. 1. Schematic diagrams of multi-pass heat exchangers with external recycle at both ends.

equation and the corresponding boundary conditions are as follows:

$$\frac{\partial^2\psi_i(\eta_i,\xi)}{\partial\eta_i^2}=\left[\frac{W_i^2 v_i(\eta_i)}{L\alpha}\right]\frac{\partial\psi_i(\eta_i,\xi)}{\partial\xi},\quad 0\leqslant\xi\leqslant1,\ \ i=a,b,c,d \tag{5}$$

$$\psi_a(0,\xi)=0 \tag{6}$$

$$\frac{\partial\psi_a(1,\xi)}{\partial\eta_a}=-\frac{W_a}{W_b}\frac{\partial\psi_b(1,\xi)}{\partial\eta_b} \tag{7}$$

$$\frac{\partial\psi_a(1,\xi)}{\partial\eta_a}=-\frac{W_a}{W}[\psi_a(1,\xi)-\psi_b(1,\xi)] \tag{8}$$

$$\frac{\partial\psi_b(0,\xi)}{\partial\eta_b}=-\frac{W_b}{W_c}\frac{\partial\psi_c(0,\xi)}{\partial\eta_c} \tag{9}$$

$$\frac{\partial\psi_b(0,\xi)}{\partial\eta_b}=-\frac{W_b}{W}[\psi_b(0,\xi)-\psi_c(0,\xi)] \tag{10}$$

$$\frac{\partial\psi_c(1,\xi)}{\partial\eta_c}=-\frac{W_c}{W_d}\frac{\partial\psi_d(1,\xi)}{\partial\eta_d} \tag{11}$$

$$\frac{\partial\psi_c(1,\xi)}{\partial\eta_c}=-\frac{W_c}{W}[\psi_c(1,\xi)-\psi_d(1,\xi)] \tag{12}$$

$$\psi_d(0,\xi)=0 \tag{13}$$

Substituting the velocity profiles in to the governing equation and using the method of separation variables, one can get

$$\psi_i(\eta_i,\xi)=\sum_{m=0}^{\infty}S_{i,m}F_{i,m}(\eta_i)G_m(\xi),\quad 0\leqslant\xi\leqslant1,\ \ i=a,b,c,d \tag{14}$$

where

$$G_m(\xi)=e^{-\lambda_m(1-\xi)},\quad 0\leqslant\xi\leqslant1 \tag{15}$$

$$F''_{i,m}(\eta_i)-\left[\frac{\lambda_m W_i^2 v_i(\eta_i)}{L\alpha}\right]F_{i,m}(\eta_i)=0,\quad 0\leqslant\eta_i\leqslant1,\ \ i=a,b,c,d \tag{16}$$

By following the same calculation procedure performed in our previous work [31], the dimensionless outlet temperature for multi-pass devices (θ_F) can be obtained in terms of the Graetz number (Gz), eigenvalues (λ_m), expansion coefficients ($S_{a,m}, S_{b,m}, S_{c,m}$, and $S_{d,m}$), and eigenfunctions ($F_{a,m}(\eta_a)$, $F_{b,m}(\eta_b)$ $F_{c,m}(\eta_c)$ and $F_{d,m}(\eta_d)$). The eigenvalues ($\lambda_1,\lambda_2,\ldots,\lambda_m,\ldots$) can be calculated from the following equations:

$$\frac{F_{a,m}(1)}{F'_{a,m}(1)}=-\frac{W_bF_{b,m}(1)}{W_aF'_{b,m}(1)} \tag{17}$$

$$\frac{F_{b,m}(0)}{F'_{b,m}(0)}=-\frac{W_cF_{c,m}(0)}{W_bF'_{c,m}(0)} \tag{18}$$

$$\frac{F_{c,m}(1)}{F'_{c,m}(1)}=-\frac{W_dF_{d,m}(1)}{W_cF'_{d,m}(1)} \tag{19}$$

It is easy to find the orthogonality condition as

$$\begin{aligned}&W_bW_cW_d\int_0^1\left[\frac{W_a^2v_a(\eta_a)}{L\alpha}\right]S_{a,m}S_{a,n}F_{a,n}F_{a,m}\,d\eta_a\\&+W_cW_dW_a\int_0^1\left[\frac{W_b^2v_b(\eta_b)}{L\alpha}\right]S_{b,m}S_{b,n}F_{b,n}F_{b,m}\,d\eta_b\\&+W_dW_aW_b\int_0^1\left[\frac{W_c^2v_c(\eta_c)}{L\alpha}\right]S_{c,m}S_{c,n}F_{c,n}F_{c,m}\,d\eta_c\\&+W_aW_bW_c\int_0^1\left[\frac{W_d^2v_d(\eta_d)}{L\alpha}\right]S_{d,m}S_{d,n}F_{d,n}F_{d,m}\,d\eta_d\\&=0,\quad n\neq m\end{aligned} \tag{20}$$

The average dimensionless outlet temperatures for the multi-pass devices, which are referred to the bulk temperature, are obtained from the overall energy balances around each subchannels. The results are

$$\begin{aligned}\psi_{F,ab}&=\frac{-\int_0^1 v_bW_bB\psi_b(\eta_b,0)\,d\eta_b}{V(R+1)}\\&=\frac{-2W}{(R+1)W_bGz}\sum_{m=0}^{\infty}\frac{e^{-\lambda_m}S_{b,m}}{\lambda_m}\{F'_{b,m}(1)-F'_{b,m}(0)\}\end{aligned} \tag{21}$$

or

$$\begin{aligned}\psi_{F,cd}&=\frac{-\int_0^1 v_cW_cB\psi_c(\eta_c,0)\,d\eta_c}{V(R+1)}\\&=\frac{-2W}{(R+1)W_cGz}\sum_{m=0}^{\infty}\frac{e^{-\lambda_m}S_{c,m}}{\lambda_m}\{F'_{c,m}(1)-F'_{c,m}(0)\}\end{aligned} \tag{22}$$

Moreover, the sum of the two average dimensionless outlet temperatures can be examined by making the overall energy balance through the whole conduit as following

$$\begin{aligned}&V(1-\psi_{F,ab})+V(1-\psi_{F,cd})\\&=\int_0^1\frac{\alpha BL}{W_a}\frac{\partial\psi_a(0,\xi)}{\partial\eta_a}\,d\xi+\int_0^1\frac{\alpha BL}{W_d}\frac{\partial\psi_d(0,\xi)}{\partial\eta_d}\,d\xi\end{aligned} \tag{23}$$

where the left-hand-side term refers to the net outlet energy while the right-hand-side term is the total amount of heat transfer from the walls to the fluid. Eq. (23) can be rewritten in the form of

$$\psi_{\mathrm{F,ab}} + \psi_{\mathrm{F,cd}} = 2 - \frac{2}{Gz}\left[\sum_{m=0}^{\infty} S_{\mathrm{a},m}F'_{\mathrm{a},m}(0)\frac{(1-\mathrm{e}^{-\lambda_m})W}{\lambda_m W_\mathrm{a}} + \sum_{m=0}^{\infty} S_{\mathrm{d},m}F'_{\mathrm{d},m}(0)\frac{(1-\mathrm{e}^{-\lambda_m})W}{\lambda_m W_\mathrm{d}}\right] \tag{24}$$

Similarly, the average dimensionless outlet temperatures for the single-pass and double-pass devices are calculated by Eqs. (25) and (26), respectively.

$$\theta_{0,\mathrm{F}} = 1 - \psi_{0,\mathrm{F}} = \frac{1}{Gz}\sum_{m=0}^{\infty}\left[\frac{(1-\mathrm{e}^{-\lambda_{0,m}})}{\lambda_{0,m}}S_{0,m}F'_{0,m}(0) - \frac{(1-\mathrm{e}^{-\lambda_{0,m}})}{\lambda_{0,m}}S_{0,m}F'_{0,m}(1)\right] \tag{25}$$

$$\theta_{\mathrm{D,F}} = 1 - \psi_{\mathrm{D,F}} = \frac{1}{Gz}\left[\sum_{m=0}^{\infty}\frac{(1-\mathrm{e}^{-\lambda_{\mathrm{D},m}})}{\lambda_{\mathrm{D},m}}\frac{W}{W_\mathrm{a}}S_{\mathrm{A},m}F'_{\mathrm{A},m}(0) + \sum_{m=0}^{\infty}\frac{(1-\mathrm{e}^{-\lambda_{\mathrm{D},m}})}{\lambda_{\mathrm{D},m}}\frac{W}{W_\mathrm{b}}S_{\mathrm{B},m}F'_{\mathrm{B},m}(0)\right] \tag{26}$$

3. Heat transfer efficiency improvement

The Nusselt number for a multi-pass device with external recycle by following the same mathematical treatment performed in our previous work [31] was thus calculated as follows:

$$\overline{Nu} = \frac{\bar{h}W}{k} = \frac{2V}{2\alpha BL}(1-\psi_\mathrm{F}) = \frac{1}{2}Gz(1-\psi_\mathrm{F}) = 0.5Gz\theta_\mathrm{F} \tag{27}$$

Similarly, for the single-pass device and double-pass device

$$\overline{Nu_\mathrm{D}} = \frac{\overline{h_\mathrm{D}}W}{k} = \frac{2VW}{2\alpha BL}(1-\psi_{\mathrm{D,F}}) = \frac{1}{2}Gz(1-\psi_{\mathrm{D,F}}) = 0.5Gz\theta_{\mathrm{D,F}} \tag{28}$$

$$\overline{Nu_0} = \frac{\overline{h_\mathrm{D}}W}{k} = \frac{2VW}{2\alpha BL}(1-\psi_{0,\mathrm{F}}) = \frac{1}{2}Gz(1-\psi_{0,\mathrm{F}}) = 0.5Gz\theta_{0,\mathrm{F}} \tag{29}$$

Two definitions of heat-transfer efficiency improvements are presented in this study. One is the percentage increase, I_{h1} (%), in the heat transfer rate base on that of a single-pass operation without recycle under the same working dimension and operating conditions, as shown in Eq. (30)

$$I_{\mathrm{h1}}(\%) = \frac{\overline{Nu} - \overline{Nu_0}}{\overline{Nu_0}} \times 100\% = \frac{\psi_{0,\mathrm{F}} - \psi_\mathrm{F}}{1-\psi_{0\mathrm{F}}} \times 100\% = \frac{\theta_{\mathrm{F}} - \theta_{0,\mathrm{F}}}{\theta_{0,\mathrm{F}}} \times 100\% \tag{30}$$

The other is the percentage increase, I_{h2} (%), in the heat transfer rate base on that of our previous work [31] with the same working dimension and operating conditions, except for the recycle type, as shown in Eq. (31)

$$I_{\mathrm{h2}}(\%) = \frac{\overline{Nu} - \overline{Nu}_{\mathrm{prev.}}}{\overline{Nu}_{\mathrm{prev.}}} \times 100\% = \frac{\psi_{\mathrm{prev.,F}} - \psi_\mathrm{F}}{1-\psi_{\mathrm{prev.,F}}} \times 100\% = \frac{\theta_\mathrm{F} - \theta_{\mathrm{prev.,F}}}{\theta_{\mathrm{prev.,F}}} \times 100\% \tag{31}$$

3.1. The power consumption increment

By assuming the laminar flow in the each conduit, the friction loss in conduits may be estimated by assuming only the friction loss to the walls were significant

$$\ell w_\mathrm{f} = \frac{2f\bar{v}^2L}{D_\mathrm{e}} \tag{32}$$

where the friction factor is $f = 24/Re$. Moreover, the power consumption increment, I_p, due to the friction losses ($\ell w_{\mathrm{f,a}}, \ell w_{\mathrm{f,b}}, \ell w_{\mathrm{f,c}}$ and $\ell w_{\mathrm{f,d}}$ for the multi-pass devices while $\ell w_{\mathrm{f},0}$ for the single-pass device) in the conduits can be readily defined as

$$I_\mathrm{p} = \frac{P-P_0}{P_0} = \frac{(R+1)(\ell w_{\mathrm{f,a}} + \ell w_{\mathrm{f,b}} + \ell w_{\mathrm{f,c}} + \ell w_{\mathrm{f,d}}) - (2\ell w_{\mathrm{f},0})}{2\ell w_{\mathrm{f},0}} \tag{33}$$

$$= \frac{1}{2}(R+1)^2\left(\frac{W}{W_\mathrm{a}}\right)^3 + \frac{1}{2}(R+1)^2\left(\frac{W}{W_\mathrm{b}}\right)^3 - 1 \tag{34}$$

4. Results and discussion

The mathematical treatment and calculation procedure in the present study are quite similar to those obtained in our previous work [31], except the recycle type. The theoretical results of the present study are not only compared to the single-and double-pass devices but also to our previous work [31] to confirm the device performance improvement of the present new recycle type. The influences of the recycle ratio R, Graetz number Gz and subchannel thickness ratio β on the mixed inlet temperature have the same tendency as those in our previous work [31]. The mixed inlet temperature is proportional to the recycle ratio R but it is inverse proportional to the Graetz number Gz and channel thickness ratio β. Fig. 2 shows the outlet temperature θ_F vs. Graetz number Gz with the subchannel thickness ratio β as a parameter under $R = 1$ and 5. The outlet temperature θ_F increases with increasing the recycle ratio R and with decreasing the channel thickness ratio β and Graetz number Gz.

Two conflict effects on heat transfer efficiency are produced by applying the recycle-effect concept to the multi-pass heat exchangers. The advantage effect is the heat-transfer convection coefficient increment due to the fluid velocity increases with increasing the recycle ratio as shown in Eqs. (1)–(4). On the other hand, the disadvantage effect

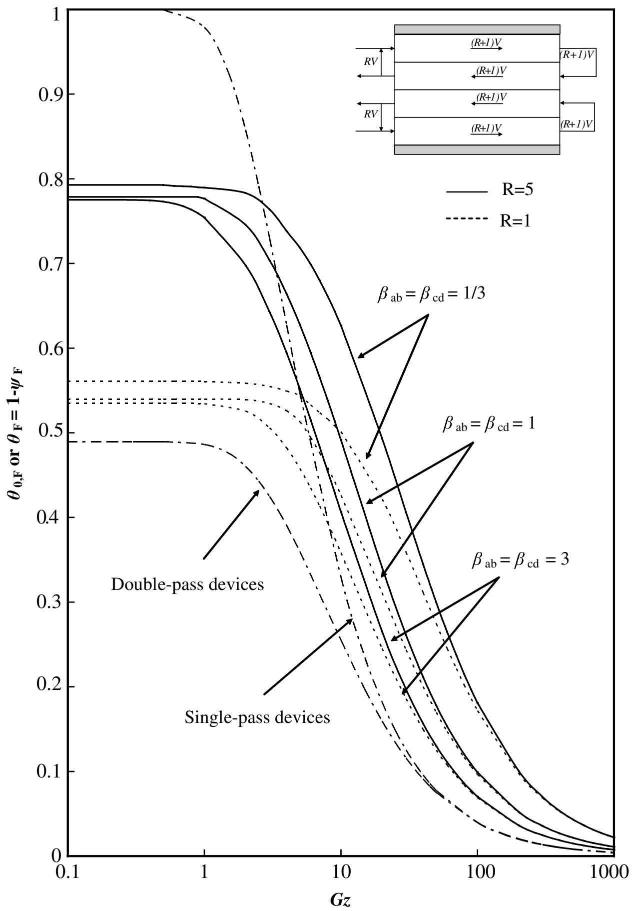

Fig. 2. Outlet temperature θ_F vs. Gz with the channel thickness ratio as a parameter; $R = 1$ and 5.

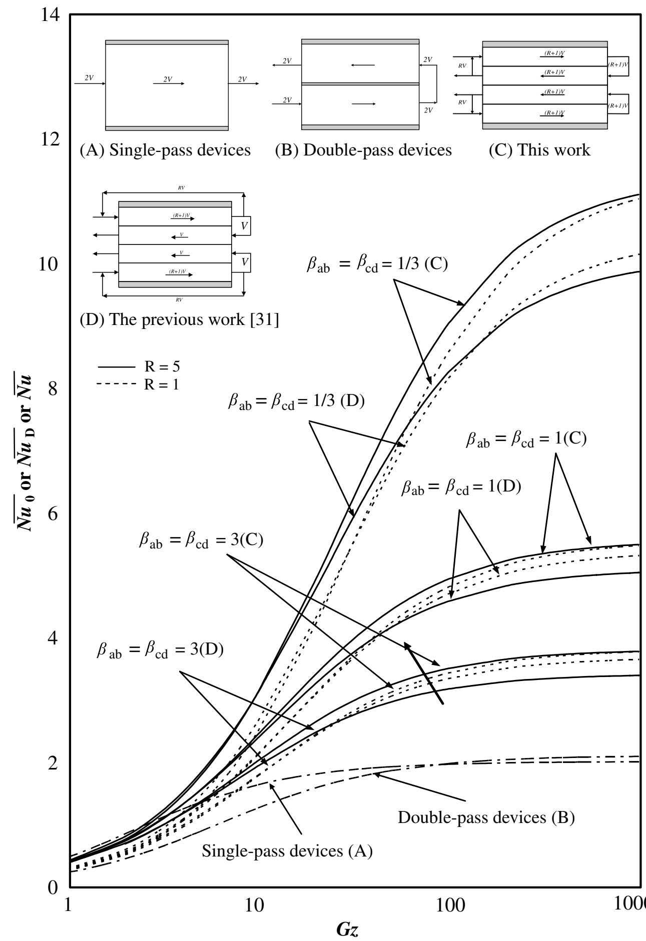

Fig. 3. The comparison of average Nusselt number obtained in the present and previous studies with β_{ab} (or β_{cd}) as a parameter; $R = 1$ and 5.

is the driving force decrement (the temperature difference between the two outer walls and flowing fluid) owing to the inlet fluid premixes with the recycle fluid with higher temperature. The heat-transfer efficiency improvement is thus achieved while the advantage effect overcomes the disadvantage one, and this is the value of the present study. A Nusselt number can be used to measure the convection heat transfer occurring at the wall surface [36]. An average Nusselt number is defined in Eq. (27) for the multi-pass devices in this study while the Eqs. (28) and (29) are the definitions of average Nusselt number for double-and single-pass devices, respectively. The comparisons of the average Nusselt number of this work to the previous work and single-and double-pass devices are shown in Fig. 3. Because of the average Nusselt number $\overline{Nu}$ proportions to the outlet temperature θ_F as indicated in Eq. (27), the influences of the recycle ratio R and channel thickness ratio β on the $\overline{Nu}$ has the same tendency as those on the θ_F. However, the Eq. (27) shows that the average Nusselt number $\overline{Nu}$ is not only proportional to the θ_F but also to Graetz number Gz and thus, $\overline{Nu}$ increases with increasing Gz as shown in Fig. 3. Fig. 3 also indicates that the $\overline{Nu}$ in this study is higher than that in previous work [31] under high Graetz numbers, say $Gz > 30$. The results show that the recycle type in this work is preferred rather than that in the previous work [31] in high Graetz number.

Two heat-transfer efficiency improvements, say I_{h1} and I_{h2}, are represented in Tables 1 and 2, respectively. The heat-transfer efficiency improvement I_{h1} shows the percentage increase in heat transfer rate based on that of a single-pass operation without external recycle under the same working dimensions and operating conditions while the percentage increase in heat transfer rate based on that of the previous work [31] is referred to I_{h2}. Table 1 shows that the I_{h1} increases with increasing recycle ratio R but decreases with increasing the channel thickness ratio β. The minus sign in Table 1 shows that the single-pass heat exchanger without external recycle is preferred rather than using the multi-pass device even with external recycle. The heat-transfer efficiency improvement of the new recycle type in the present work is illustrated in Table 2, as compared to the previous work [31]. It is readily confirmed from Table 2 that the heat-transfer efficiency of the new recycle type of this work is better than that of the previous work [31] for large Graetz number. In contrast, the recycle type of the previous work is preferred rather than the new recycle type of this work while a multi-pass heat exchanger is operated in the low Graetz number region.

Table 1
The heat-transfer efficiency improvement I_{h1} with recycle ratio and channel thickness ratio as parameters

I_{h1} (%)	$R = 1$			$R = 5$		
	β_{ab} (or β_{cd})			β_{ab} (or β_{cd})		
	1/3	1	3	1/3	1	3
$Gz = 1$	−44.86	−42.74	−45.41	−20.48	−19.97	−22.94
10	52.18	29.38	8.72	90.24	49.17	23.42
100	334.33	143.76	74.07	357.62	150.18	77.67
1000	448.18	172.14	87.49	451.66	172.92	87.91

Table 2
The heat-transfer efficiency improvement I_{h2} with recycle ratio and channel thickness ratio as parameters

I_{h1} (%)	$R = 1$			$R = 5$		
	β_{ab} (or β_{cd})			β_{ab} (or β_{cd})		
	1/3	1	3	1/3	1	3
$Gz = 1$	−11.15	−3.85	−5.18	−6.79	−3.58	−4.05
10	−6.12	−0.723	−0.57	0.16	2.37	4.28
100	5.11	2.36	2.72	9.45	7.73	10.28
1000	8.77	3.04	3.33	12.53	8.90	11.37

Table 3
The power consumption increment with recycle ratio and channel thickness ratio as parameters

R	I_p		
	$\beta_{ab} = \beta_{cd} = 1/3$	$\beta_{ab} = \beta_{cd} = 1$	$\beta_{ab} = \beta_{cd} = 3$
0.5	596.4	143	596.4
1.0	1061.1	255	1061.1
2.0	2388.7	575	2388.7
5.0	9521.6	2303	9521.6

In addition, the multi-pass operation with external recycle not only increases the heat transfer rate but also increases the power consumption of the flowing fluid in the conduit. As an illustration, the power consumption of a single-pass device was calculated by using the following working dimensions: $L = 1.2$ m, $W = 0.04$ m, $B = 0.2$ m, $V = 1 \times 10^{-5}\ \mathrm{m^3/s}$, $\mu = 8.94 \times 10^{-4}$ kg/m s, $\rho = 997.08\ \mathrm{kg/m^3}$. From these numerical values, the friction loss in an open conduit was obtained

$$P_0 = 2V\rho(\ell w_{f,0}) = 1.073 \times 10^{-4}\ \mathrm{W} = 1.44 \times 10^{-7}\ \mathrm{hp} \quad (35)$$

The power consumption increment I_p is defined in Eq. (33) and the calculated results are shown in Table 3. The power consumption increment does not depend on the Graetz number, but increases with increasing the recycle ratio R as observed from Table 3. Moreover, as shown in Table 3, the values of I_p increase with the channel thickness ratio β_{ab} (or β_{cd}) moving away from 1 and are symmetry to $\beta_{ab} = \beta_{cd} = 1$. Though the maximum value of I_p in Table 3 is 9521.6 for $R = 5$ and $\beta_{ab} = \beta_{cd} = 1/3$ (or $\beta_{ab} = \beta_{cd} = 3$), the theoretical prediction of power consumption under these conditions, say $P = 1.37 \times 10^{-3}$ hp, is still small. Fortunately, it seems reasonably to ignore the power consumption of multi-pass operations with external recycle.

5. Conclusion

A new recycle type of the multi-pass heat exchanger is designed and developed in the present study. This study is an extension of the previous work [31] and the analytical solution was obtained by following the similar mathematical treatment and calculation procedure in the previous work [31]. The theoretical results show that the multi-pass device with external recycle can enhance the heat transfer rate especially for large Gz, high R and small β. As compared to the previous study [31], the new recycle type in the present study results in a better device performance under the same working dimensions for high Graetz number, say $Gz > 30$, however, for low Graetz number, say $Gz \leqslant 30$, the recycle type in previous work [31] is preferred.

It is apparent that the mathematical formulations developed in this study may be also applied to other conjugated Graetz problems in heat-or mass-transfer devices for each particular boundary condition.

Acknowledgements

The authors thank the National Science Council of the Republic of China for its financial support.

References

[1] L. Graetz, Über die warmeleitungsfahigkeit von flussigkeiten, Ann. Phys. Chem. 25 (1885) 337–357.
[2] R.K. Shah, A.L. London, Laminar Flow Forced Convection in Ducts, Academic Press, New York, 1978, pp. 196–207.
[3] V.-D. Dang, M. Steinberg, Convective diffusion with homogeneous and heterogeneous reaction in a tube, J. Phys. Chem. 84 (1980) 214–219.
[4] P.A. Ramachandran, Boundary integral solution method for the Graetz problem, Numer. Heat Transfer, Part B 23 (1993) 257–268.
[5] R.F. Barron, X. Wang, R.O. Warrington, T. Ameel, Evaluation of the eigenvalues for the Graetz problem in slip-flow, Int. Commun. Heat Mass Transfer 23 (1996) 563–574.
[6] E. Papoutsakis, D. Ramkrishna, H.C. Lim, The extended Graetz problem with prescribed wall flux, AIChE J 26 (1980) 779–787.
[7] C.T. Liou, F.S. Wang, Solutions to the extended Graetz problem for a power-model fluid with viscous dissipation and different entrance boundary conditions, Numer. Heat Transfer 17 (1990) 91–108.
[8] S. Bilir, Numerical solution of Graetz problem with axial conduction, Numer. Heat Transfer, Part A 21 (1992) 493–500.
[9] B. Weigand, An extract analytical solution for the extended turbulent Graetz problem with Dirichlet wall boundary conditions for pipe and channel flows, Int. J. Heat Mass Transfer 39 (1996) 1625–1637.
[10] J. Lahjomri, A. Oubarra, A. Alemany, Heat transfer by laminar Hartmann flow in thermal entrance region with a step change in wall temperatures: the Graetz problem extended, Int. J. Heat Mass Transfer 45 (2002) 1127–1148.
[11] E.J. Davis, S. Venkatesh, The solution of conjugated multiphase heat and mass transfer problems, Chem. Eng. Sci. 34 (1979) 775–787.
[12] E. Papoutsakis, D. Ramkrishna, Conjugated Graetz problems. Part I: General formalism and a class of solid–fluid problems, Chem. Eng. Sci. 36 (1981) 1381–1390.

[13] E. Papoutsakis, D. Ramkrishna, Conjugated Graetz problems. Part II: Fluid–fluid problems, Chem. Eng. Sci. 36 (1981) 1393–1399.
[14] X. Yin, H.H. Bau, The conjugated Graetz problem with axial conduction, Trans. ASME 118 (1996) 482–485.
[15] C.D. Ho, W.Y. Yang, Heat transfer of conjugated Graetz problems with laminar counterflow in double-pass concentric circular heat exchangers, Int. J. Heat Mass Transfer 48 (2005) 4474–4480.
[16] C.D. Ho, H.M. Yeh, W.S. Sheu, An analytical study of heat and mass transfer through a parallel-plate channel with recycle, Int. J. Heat Mass Transfer 41 (1998) 2589–2599.
[17] C.D. Ho, C.L. Ho, Improvement in performance of double-pass concentric circular mass exchangers, J. Chem. Eng. Jpn. 36 (2003) 81–91.
[18] M. Sato, M. Goto, Gas bbsorption in water with microchannel devices, Separ. Sci. Technol. 39 (2004) 3163–3167.
[19] X.F. Peng, G.P. Peterson, Forced convection heat transfer of single-phase binary mixtures through microchannels, Exp. Therm. Fluid Sci. 12 (1996) 98–104.
[20] H.M. Yeh, C.L. Chen, Y.Y. Peng, C.H. Chen, Effect of recycle type on solvent extraction through a parallel-plate membrane module, J. Membr. Sci. 183 (2001) 109.
[21] C.D. Ho, H.M. Yeh, J.J. Guo, An analytical study on the enrichment of heavy water in the continuous thermal diffusion column with external refluxes, Separ. Sci. Technol. 37 (2002) 3129–3153.
[22] S. Curcio, V. Calabro, G. Iorio, A theoretical and experimental analysis of a membrane bioreactor performance in recycle configuration, J. Membr. Sci. 273 (2006) 129–142.
[23] N. Al-Bastaki, A. Abbas, Permeate recycle to improve the performance of a spiral-wound RO plant, Desalination 58 (2003) 119–126.
[24] V. Evren, T. Cagatay, A.R. Ozdural, Carbon dioxide-air mixtures: mass transfer in recycling packed-bed absorption columns operating under high liquid flow rates, Separ. Purif. Technol. 17 (1999) 89–96.
[25] C.D. Ho, H.M. Yeh, J.J. Guo, An analytical study on the enrichment of heavy water in the continuous thermal diffusion column with external refluxes, Separ. Sci. Technol. 37 (2002) 3129–3153.
[26] M.H. Siegel, J.C. Merchuk, K. Schugerl, Air-lift reactor analysis: interrelationships between riser, downcomer, and gas–liquid separator behavior, including gas recirculation effects, AIChE J. 32 (1986) 1585–1595.
[27] D. Kundu, A. Haji-Sheikh, D.Y.S. Lou, Heat transfer predictions in cross flow over cylinders between two parallel plates, Numer. Heat Transfer, Part A 19 (1991) 361–377.
[28] C.H. Huang, M.N. Özişik, Inverse problem of determining unknown wall heat flux in laminar flow through a parallel plate duct, Numer. Heat Transfer, Part A 21 (1992) 55–70.
[29] A.V. Kuznetsov, L. Chang, M. Xiong, Effects of thermal dispersion and turbulence in forced convection in a composite parallel-plate channel: investigation of constant wall heat flux and constant wall temperature cases, Numer. Heat Transfer, Part A 42 (2002) 365–383.
[30] G. Maranzana, I. Perry, D. Maillet, Modeling of conjugated heat transfer between parallel olates separated by a hydrodynamically developed laminar flow by the quadrupole method, Numer. Heat Transfer, Part A 46 (2004) 147–165.
[31] C.D. Ho, H.M. Yeh, Y.C. Tsai, Improvement in performance of multi-pass laminar counterflow heat exchangers with external refluxes, Int. J. Heat Mass Transfer 45 (2002) 3529–3547.
[32] G.M. Brown, Heat or mass transfer in a fluid in laminar flow in a circular or flat conduit, AIChE J. 6 (1960) 179–183.
[33] R.J. Nunge, W.N. Gill, An analytical study of laminar counterflow double-pipe heat exchangers, AIChE J. 12 (1966) 279–289.
[34] H.M. Yeh, S.W. Tsai, C.S. Lin, A study of the separation efficiency in thermal diffusion columns with a vertical permeable barrier, AIChE J. 32 (1986) 971–980.
[35] C.D. Ho, H.M. Yeh, W.S. Sheu, An analytical study of heat and mass transfer through a parallel-plate channel with recycle, Int. J. Heat Mass Transfer 41 (1998) 2589–2599.
[36] D.P.D. Incropera, Fundamentals of Heat and Mass Transfer, third ed., John & Sons, New York, 1990, pp. 314.